Original Article

Comparative pharmacokinetics of six components in normal and rheumatoid arthritis rats after intragastrical administration of Qianghuo Shengshi Decoction granules by LC-MS/MS

Xin Li [a,b,c,1], Min Wang [a,b,c,1], Yuhong Zhong [a,b,c], Qianqian Yin [a,b,c], Zheming Hu [a,b,c], Wenli Tian [a,b,c], Zhongyan Liu [a,b,c], Zhidong Liu [a,b,c,*]

[a] Engineering Research Center of Modern Chinese Medicine Discovery and Preparation Technique, Ministry of Education, Tianjin University of Traditional Chinese Medicine, Tianjin 301617, China
[b] State Key Laboratory of Component-based Chinese Medicine, Tianjin University of Traditional Chinese Medicine, Tianjin 301617, China
[c] Haihe Laboratory of Modern Chinese Medicine, Tianjin University of Traditional Chinese Medicine, Tianjin 301617, China

ARTICLE INFO

ABSTRACT

Objective: To investigate the plasma pharmacokinetics of six representative components (nodakenin, osthole, 5-*O*-methylvisammioside, ferulic acid, liquiritigenin, and liquiritin), which were the ingredients of Qianghuo Shengshi Decoction (QSD) granules, in normal and rheumatoid arthritis (RA) rats administrated QSD granules intragastrically.
Methods: A rapid and accurate ultra-high performance liquid chromatography-tandem mass spectrometry (LC-MS/MS) method was developed for the simultaneous determination of six components in plasma, and it showed a good specificity, linearity, intra-day and inter-day precision, intra-day and inter-day accuracy, extraction recovery, stability, and the less matrix effect.
Results: The validated LC-MS/MS method was successfully used to compare the plasma pharmacokinetics of six ingredients between normal and RA rats after intragastrical administration of QSD granules and differences in the pharmacokinetics were found in two types of rats. The absorption rate in the RA rats was lower for nodakenin, osthole, 5-*O*-methylvisammioside, liquiritigenin and liquiritin than in the normal group, while the absorption rate of ferulic acid remained constant in two groups. In comparison with the normal rats, the exposure concentration of nodakenin was higher and that of other five components except for nodakenin was lower under pathological conditions. Additionally, the absorptive amount of nodakenin, osthole, 5-*O*-methylvisammioside and liquiritin was increased and that of ferulic acid and liquiritigenin was reduced in the RA rats than in the normal rats. Compared with the normal rats, the retention time of nodakenin, ferulic acid and liquiritin was reduced *in vivo*, whereas the retention time of osthole, 5-*O*-methylvisammioside and liquiritigenin was raised in the body for the RA rats. In contrast to the normal rats, the data demonstrated an increase in the elimination velocity of nodakenin and a decrease in the elimination velocity of the other five components except for nodakenin in the pathological state.
Conclusion: This study showed that the pharmacokinetic behavior of the six components, nodakenin, osthole, 5-*O*-methylvisammioside, ferulic acid, liquiritigenin, and liquiritin, is different *in vivo* between normal and pathological states of rats, and this research provided the necessary experimental data to explain the pharmacokinetics of QSD granules in both normal and pathological states and provide some references for its clinical application at some level.

1. Introduction

Rheumatoid arthritis (RA) is a chronic, complex autoimmune inflammatory disease with systemic sequelae and is characterized by inflammatory changes in joint synovial tissues, cartilage, bones, and extra-articular sites, leading to cartilage destruction, bone erosion, and disability (Smolen, Aletaha, & McInnes, 2016). Traditional Chinese medicines (TCMs) have been widely used clinically in the treatment of RA, with definite, significant therapeutic effects, minimal toxicity and limited side effects (Zhang et al., 2022a; Zhang et al., 2022b). Studies have suggested that various TCM extracts, single herb, and prescriptions exert therapeutic effects on RA primarily by inhibiting the proliferation of abnormal immune cells

and inflammatory factors, regulating the immune system, and reducing angiogenesis, etc. (He et al., 2021; Ma et al., 2023; Xie et al., 2021). Qianghuo Shengshi Decoction (QSD) has clear anti-inflammatory and analgesic effects on the organism by regulating the expression of the mitogen-activated protein kinases (MAPKs) / cAMP response element-binding protein (CREB) signaling pathway (Hu et al., 2022), and QSD has been widely used to treat a variety of inflammatory and pain diseases, including RA (Dong et al., 2018).

QSD is a classic formula used to treat cold, migraine, cervical spondylosis, RA, periarthritis of shoulder and other diseases (Dong et al., 2018). QSD comes from *The Treatise on Differentiation of Internal and External Injuries* (Jin, Dongyuan Li), and is composed of *Notopterygii Rhizoma* et *Radix* (Qianghuo in Chinese), *Angelicae Pubescentis Radix* (Duhuo in Chinese), *Ligustici Rhizoma* et *Radix* (Gaoben in Chinese), *Chuanxiong Rhizoma* (Chuanxiong in Chinese), *Saposhnikoviae Radix* (Fangfeng in Chinese), *Glycyrrhizae Radix* et *Rhizoma* (Gancao in Chinese), *Viticis Fructus* (Manjingzi in Chinese). Traditional Chinese medical science believes that the integrated regulation of multi-component and multi-target is the way to exert the curative effect of TCM. The active chemical components are the pharmacodynamic material basis of TCM (Meng et al., 2022), and their discoveries are an important mission in the quality control of TCM compound and single herb. According to previous studies, the six components (nodakenin, osthole, 5-*O*-methylvisammioside, ferulic acid, liquiritigenin, and liquiritin) in QSD are the pharmacodyamic material basis for coming up to better therapeutic effects. Nodakenin, an active ingredients in *Notopterygii Rhizoma* et *Radix* (Zhang et al., 2023), has the effects of anticancer (Kim, 2023), anti-inflammation (Lim, Lee, Yun, Lee, & Kim, 2021; Yi et al., 2022; Liao et al., 2020), improving memory (Gao et al., 2015), etc. Osthole (Yang et al., 2019; Ren, Lv, & Xu, 2022), a compound seperated from *Angelicae Pubescentis Radix*, provides pharmacological effects of immune regulation and has a hepatoprotective function in treating metabolic diseases, and it can improve disease damage (Liu, Chiu, Fu, & Huang, 2015) by reducing cell oxidation and inhibiting inflammatory factors. 5-*O*-methylvisammioside, an active ingredient in *Saposhnikoviae Radix*, can provide the effects of anti-inflammation (Meng, Gao, Liu, Zheng, & Jia, 2023), anti-tumor (Wang, Liang, Cao, & Ye, 2008) and inhibition of depression (Sun et al., 2020). Ferulic acid (Li et al., 2021) exists in many TCMs including *Notopterygii Rhizoma* et *Radix*, *Ligustici Rhizoma* et *Radix* and *Chuanxiong Rhizoma*, and it can play great potential in anti-inflammatory, anti-fibrosis, ant-apoptotic, anti-aging and antioxidant activities. Both liquiritigenin and liquiritin are representative active ingredients of *Glycyrrhizae Radix* et *Rhizoma* and they have the effects of anti-inflammation (Jiang et al., 2022), inhibitory activity for tetanic contractions (Lee, Omiya, Yuzurihara, Kase, & Kobayashi, 2013), anti-tumor (Wei, Jiang, Gao, & Gao, 2017; Meng & Lin, 2019), and can relieve liver injury and inflammatory injury (Chen et al., 2019). Thus, six active ingredients, namely, nodakenin, osthole, 5-*O*-methylvisammioside, ferulic acid, liquiritigenin and liquiritin, were selected and determined in this study.

Traditional decoction has the advantages of rapid curative effect, less toxicity and minor side effect, which is the dosage form used the most widely in TCM treatment. However, it also has shortcomings, such as short shelf life, inconvenient storage and transportation, and poor compliance for the patient, which limits the application of QSD and obstructs its modern development (Lin, 2019). With the rapid development of modern TCM, granules have become one of the prominent dosage forms in TCM treatment circles, as they bring great convenience to patients to compensate for the decoction's disadvantages (Cui et al., 2022; Zhang et al., 2022a; Zhang et al., 2022b). So far, numerous studies have been conducted on the clinical application of QSD, but related reports on the quality control and new formulation development are still lacking. Therefore, in this research, we used modern techniques to prepare QSD granules and guarantee their quality.

The ingredients of TCM are numerous and complicated, and its mode of action is characterized by multi-target and multi-component, which results in its pleiotropy, peculiarity, and complexity and makes it different from chemical drugs in pharmacokinetics (Li et al., 2015). There are a number of studies on the pharmacokinetics of a single component in a single herb in China. In recent years, pharmacokinetic studies of medicine made of two or more ingredients have already gained considerably additional attention due to the continuous development and in-depth research on TCM modernization at home and abroad. The pharmacokinetics of effective components for QSD orally entering the body have not been elucidated at present, which hinders the in-depth investigations of the mechanism. In addition, pharmacokinetics is different in physiological and pathological states (Liu, Zeng, Zhou, Zhang, & Nie, 2022; Zhang et al., 2018; Xu et al., 2019), and pharmacokinetics under pathological conditions can provide more relevant information than in normal conditions. Therefore, this study compared the pharmacokinetics of six active components, nodakenin, osthole, 5-*O*-methylvisammioside, ferulic acid, liquiritigenin and liquiritin, in QSD granules in normal and RA rats using the ultra-high performance liquid chromatography-tandem mass spectrometry (LC-MS/MS) method to provide more significant information for clinical practice.

2. Materials and methods

2.1. Materials and reagents

Notopterygii Rhizoma et *Radix* (Lot No.: 10701501, Sichuan, China), *Angelicae Pubescentis Radix* (Lot No.: 10701501, Gansu, China), *Ligustici Rhizoma* et *Radix* (Lot No.: 10701501, Sichuan, China), *Chuanxiong Rhizoma* (Lot No.: 10701501, Hebei, China), *Saposhnikoviae Radix* (Lot No.: 10701501, Liaoning, China), *Glycyrrhizae Radix* et *Rhizoma* (Lot No.: 10701501, Gansu, China) and *Viticis Fructus* (Lot No.: 10701501, Jiangxi, China) were provided by Heilongjiang Zhenbaodao Pharmaceutical Co., Ltd. (Jixi, China), identified by Dongli Qi, an associate professor of Tianjin University of TCM, and met requirements of the *Chinese Pharmacopoeia* (Edition 2020). Nodakenin (Lot No.: 102835, 98%) was purchased from Jiangsu Yongjian Pharmaceutical Technology Co., Ltd. (Taizhou, China). Osthole (Lot No.: 110822-201710, 99.5%), ferulic acid (Lot No.: 110773-201614, 99.0%), 5-*O*-methylvisammioside (Lot No.: 11153-201811, 97.4%) and carbamazepine (Lot No.: 100142-201706, 100%) were purchased from China National Institutes for Food and Drug Control (Beijing, China). Liquiritin (Lot No.: 213J11X108109, 98%) and liquiritigenin (Lot No.: C26A10O87040, 98%) were purchased from Shanghai Yuanye Biotechnology Co., Ltd. (Shanghai, China). Formic acid (Lot No.: A3MMC-UV, LC-MS > 98%) was purchased from TCI Shanghai Chemical Industry Development Co., Ltd. (Shanghai, China). Acetonitrile (Lot No.: 212522) and methanol (Lot No.: 214804) were obtained from Fisher Scientific Co., Ltd. (Fairlawn, NJ, USA). Dextrin (Lot No.: 20210811) was purchased from Shandong Liaocheng Ahua Pharmaceutical Co., Ltd. (Liaocheng, China). Ethanol (Lot No.: 211125) was purchased from Tianjin Concord Technology Co., Ltd. (Tianjin, China). Deionized water was produced from a Milli-Q water purification system (Millipore, Commonwealth of Massachusetts, USA).

2.2. Animals

Male Sprague-Dawley rats (180–220 g) were purchased from Beijing Huafukang Biotechnology Co., Ltd. (Beijing, China). The ani-

mal license number was SCXK (Beijing, China) 2019-0008. All animal-related experiments were approved by the animal ethics committee of Tianjin University of TCM under the review number TCM-LAEC2021197. All rats were given free access to food and water for 7 d in a barrier system of specific-pathogen-free level (temperature, 23–27 °C; relative humidity, 48%−52%; 12 h light/-dark cycle) before starting the experiment.

2.3. LC-MS/MS analysis conditions

The applied LC-MS/MS system (Agilent, City of Santa Clara, USA) was composed of an Agilent 1290 high performance liquid chromatograph, a 6460 triple quadrupole mass spectrometer equipped with an electron spray ionization (ESI) source and MassHunter B.07.00 software. The separations of six components were achieved on a BEH C_{18} column (Waters Acquity Uplc, 2.1 mm × 100 mm, 1.7 μm, Torrance, CA, USA). The column temperature was 30 °C and the injection volume was 5 μL. The mobile phases were delivered at a flow rate of 0.3 mL/min, and those consisted of 0.1% formic acid water (A) and acetonitrile (B) with the gradients: 0–5 min, 85%−80% A; 5–10 min, 80%−50% A; 10–13 min, 50%−40% A; 13–18 min, 40%−35% A; 18–18.01 min, 35%−85% A; 18.01–20 min, 85% A. Analytes were quantified by the multiple reaction monitoring (MRM) mode in both positive and negative ion detection modes. The following settings were used: the desolvation temperature, 300 °C; the gas flow rate of desolvation, 11 L/min; the nitrogen pressure, 103 421 Pa; the capillary voltage, 3 000 V. The mass spectrometry (MS) parameters of the six components and carbamazepine (Internal Standard, IS) were given in Table 1.

2.4. Standard solutions

The standards were accurately weighed and respectively dissolved in methanol to obtain the single high-concentration standard solutions. The above single standard solutions were precisely pipetted into a volumetric flask and diluted with methanol to acquire the mixed standard solutions of three concentrations (low, medium and high): nodakenin (2.100 ng/mL, 537.6 ng/mL and 806.4 ng/mL), osthole (2.562 ng/mL, 656.0 ng/mL and 984.0 ng/mL), 5-O-methylvisammioside (1.112 ng/mL, 284.8 ng/mL and 427.2 ng/mL), ferulic acid (2.350 ng/mL, 601.6 ng/mL and 902.4 ng/mL), liquiritigenin (1.260 ng/mL, 324.0 ng/mL and 486.0 ng/mL), liquiritin (1.680 ng/mL, 541.0 ng/mL and 811.5 ng/mL). The high-concentration carbamazepine (IS) solution was rigorously diluted by methanol to 1 070 ng/mL. All solutions were stored in accordance with the manufacturer's instructions.

2.5. Quality control (QC) samples, blank plasma samples and drug-containing plasma samples

QC samples: 100 μL blank plasma, 20 μL carbamazepine (1.07 μg/mL, IS) and 800 μL acetonitrile were added into 1.5 mL EP tubes containing the mixed standard solutions dried with nitrogen to get the mixture of QC at three concentrations. The mixture was vortexed for 5 min and centrifuged at 12 000 r/min for 10 min,

and then the supernatant was transferred into new EP tubes and dried with nitrogen. After re-dissolving with 100 μL the initial mobile phases, vortexing for 5 min, and centrifuging for 10 min at 12 000 r/min, the supernatant was transferred to autosampler vials for LC-MS/MS analysis. Blank plasma samples: 100 μL blank plasma and 800 μL acetonitrile were added into 1.5 mL EP tubes to get the mixture of blank plasma. The mixture was vortexed for 5 min and centrifuged at 12 000 r/min for 10 min, and then the supernatant was transferred into new EP tubes and dried with nitrogen. After re-dissolving with 100 μL the initial mobile phases, vortexing for 5 min, and centrifuging for 10 min at 12 000 r/min, the supernatant was transferred to autosampler vials for LC-MS/MS analysis. Drug-containing plasma samples: 100 μL drug-containing plasma obtained from rats after administered intragastrically, 20 μL carbamazepine (1.07 μg/mL, IS) and 800 μL acetonitrile were added into 1.5 mL EP tubes to get the mixture of drug-containing plasma. The mixture was vortexed for 5 min and centrifuged at 12 000 r/min for 10 min, and then the supernatant was transferred into new EP tubes and dried with nitrogen. After re-dissolving with 100 μL the initial mobile phases, vortexing for 5 min, and centrifuging for 10 min at 12 000 r/min, the supernatant was transferred to autosampler vials for LC-MS/MS analysis.

2.6. Preparation of QSD granules

Firstly, the QSD slices were soaked with water for 0.5 h in a ratio of 1:14 (mass to volume ratio) and extracted by the reflux apparatus for 2 h, the extracting solution was filtered through two layers of gauze into the containers. Secondly, the residue was refluxed with fresh water (mass of dried slices to volume of water ratio, 1:12) for 1 h again, subsequently, the water solution was filtered and blended with the first extracting solution. Then, the combined solution was concentrated in a rotary vacuum evaporator at 60 °C to obtain the concentrated solution (density, 1.03–1.07 g/L). After that, the QSD extract powder was prepared using a spray dryer. The QSD extract powder and dextrin were mixed in a ratio of 1:1, which were added into the mixing torque rheometer (MTR3, Caleva, UK; stirring speed, 80 r/min; stirring time, 190 s). The mixture was wet with 85% ethanol (0.25 mL/g) to make the soft materials, then they were passed through a 14 mesh sieve and dried at 60 °C for 1 h to produce QSD granules.

2.7. Method validation

2.7.1. Specificity

The chromatograms of the blank plasma, the blank plasma added standards, and the drug-containing plasma after intragastric administration were evaluated and compared to determine whether endogenous matrix components exhibited potential interferences at retention time for the six analytes and IS.

2.7.2. Linearity and lower limit of quantification (LLOQ)

The mixed standard solution was diluted with methanol to make a series of working solutions with different concentrations. The linearity of the method was assessed by testing the standards

Table 1
MS parameters of six components and carbamazepine.

Components	Precursor ion	Product ion	Fragmentor (V)	Collision energy (eV)	Ionization mode
Carbamazepine	237.0	194.0	95	16	Positive
Nodakenin	409.1	247.0	90	7	Positive
Osthole	244.9	188.9	94	8	Positive
5-O-Methylvisammioside	453.0	291.0	145	21	Positive
Ferulic acid	192.7	133.7	63	−9	Negative
Liquiritigenin	254.8	118.7	110	−20	Negative
Liquiritin	416.9	255.0	150	−15	Negative

at each concentration level. The regression equations were calculated using the concentration (x) of analytes and the peak area ratio (y) of analytes to the internal standard, which adopted a linear regression model and a weighting factor: $1/x$. LLOQ was the corresponding concentration of analytes if the ratio of signal to noise was 10:1.

2.7.3. Precision and accuracy

The QC samples of low, medium and high concentrations (n = 6) were made and measured for three consecutive days. The ratio of the peak area of each component to that of the internal standard was brought into the accompanying standard curve to calculate the concentrations used to estimate intra-day, inter-day precision and accuracy. The precision was assessed on the relative standard deviation (RSD) and RSD value was required to be no more than 15; %. The accuracy was evaluated on the relative error (RE), and RE value was required to be within ± 15%.

2.7.4. Matrix effect and extraction recovery

The matrix effect could be assessed by a ratio of the analyte peak area with matrix ions (QC samples added the extracts of blank plasma) to those without matrix ions (QC samples added the mobile phase). A total of 100 μL blank plasma, 20 μL carbamazepine (1.07 μg/mL, IS) and 800 μL acetonitrile were added into 1.5 mL EP tubes to get the mixture. The mixture was vortexed for 5 min and centrifuged at 12 000 r/min for 10 min, and then the supernatant was transferred into new EP tubes and dried with nitrogen. The mixed control solution (100 μL) that were prepared with the initial mobile phase to get the same concentration as the low, medium and high QC samples were added to the residue respectively. The mixture was vortexed for 5 min, centrifuged at 12 000 r/min for 10 min, and the supernatant was taken into the LC-MS/MS to determine the peak area (A) of each component. The mixed control solutions were diluted with mobile phase to obtain the same concentration solution as the low, medium and high QC samples, and then were added into the sample injector to test analytes' peak area (B). According to "2.5", QC samples of the low, medium and high concentrations were prepared and analyzed to determine the peak area (C) of each component. Matrix effects and recoveries were calculated as follows, and the RSD of the matrix effects and recoveries was required to be less than 15 %:

$$\text{Matrix effect}(\%) = \text{A/B} \times 100 \qquad (1)$$

$$\text{Extraction recovery}(\%) = \text{C/A} \times 100 \qquad (2)$$

2.7.5. Stability

QC samples at the low, medium and high concentrations were prepared and analyzed to explore stability evaluated by RE, and RE was required to be within ± 15%. The low-temperature stability, long-term stability, and freeze–thaw stability were respectively investigated by measuring the peak area of QC samples stored at 4 °C for 24 h, stored at −80 °C for 5 d, and stored at −80 °C and room temperature.

2.8. Pharmacokinetic study

2.8.1. RA models

Rats were randomly divided into two groups of six rats in each group: normal group was intradermally given 0.1 mL physiological saline into the left hind foot and RA group was intradermally given 0.1 mL complete Freund's adjuvant in the same position. The inflammatory degree was reflected through the scoring system of arthritis index, where no swelling of the whole foot was recorded as zero score, the redness and swelling of the toe joint were recorded as one score, the swelling of the toe joint and the plantar

was recorded as two scores, the foot swelling below the ankle joint was recorded as three scores, the swelling of the whole foot including ankle joint was recorded as four scores. A cumulative score was applied in the above system and RA models were successfully established if the score was greater than or equal to four. The inflammatory index in the normal group was zero, the rats had no symptoms of arthritis, and the rats had healthy diets, normal activities, and positive statuses. All rats in the RA group had significantly swollen feet (including ankle joints), reduced diets, fewer activities, and more fatigue, and the score of all rats was ten, which showed that the RA model was successfully established with decent reproducibility.

2.8.2. Collection of plasma samples

Rats were intramuscularly given a dose of QSD granules at 1.22 g/kg after being fasted but given access to water for 12 h. The blood samples (0.3 mL) were collected from the inner canthus of rat eyes via glass capillaries into tubes pre-treated with heparin before dosing and subsequently at 5 min, 10 min, 15 min, 30 min, 45 min, 1 h, 1.5 h, 2 h, 3 h, 4 h, 6 h, 8 h, 10 h, 12 h, 14 h, 24 h, 36 h, and 48 h, centrifuged at 5 000 r/min for 10 min. The upper plasma was stored at −80 °C and was processed according to "2.5", and the supernatant was used for LC-MS/MS analysis.

2.8.3. Data processing

Data were analyzed by the Phoenix WinNonlin software (Version 8.1.x, Pharsight, USA) and SPSS statistics software (Version 21, IBM, China). Pharmacokinetic parameters, including the half-life ($t_{1/2}$), the peak time (T_{max}), the peak concentration (C_{max}), the area under the curve ($AUC_{0-\infty}$), and the mean residence time ($MRT_{0-\infty}$), were calculated using a non-compartmental model. The data were presented as mean ± SD. A statistical analysis method, t-test, was used for the data analysis, and differences were regarded as statistically significant if P values were less than 0.05.

3. Results

3.1. Method validation

Based on the typical chromatograms of the plasma samples in Fig. 1, the results showed that there were no significant interfering peaks at the retention time of the six components, and the excellent peaks were provided by the analytical method, indicating a high specificity. The results of regression equations, linear ranges, and LLOQ for the six analytes were given in Table 2. Within the linear range, a good linearity of the method was shown for each analyte in this study ($r \geq 0.99$). The results for the intra-day and inter-day precision and the corresponding accuracy for the six analytes were summarized in Table 3. The intra-day RSD of the six components was less than 6.0%, the inter-day RSD was less than 5.0%, and the intra-day RE ranged from −4.7% to 8.4%, and the inter-day RE ranged from −7.3% to 14.1%. The intra-day and inter-day precision of all components was less than 15% and the intra-day and inter-day accuracy were within ± 15% at three QC levels. From Table 4, it could be seen that the RSD of the components' matrix effects was less than 5.8%, the RSD of the average extraction recoveries was less than 7.0%, indicating that there was no obvious matrix interference and the recoveries had a steady and reproducible performance. The stability results were presented in Table 5. RE of the QC samples in three conditions, 4 °C for 24 h, −80 °C for 5 d and three-freeze–thaw cycles, ranged from −12.01 to 12.26, indicating that the analytes could remain stable during the handling and storage of samples. In summary, the effectiveness of the bioanalytical method was proven in terms of specificity, linearity, precision and accuracy, matrix effect, recovery, and stability. Therefore, we
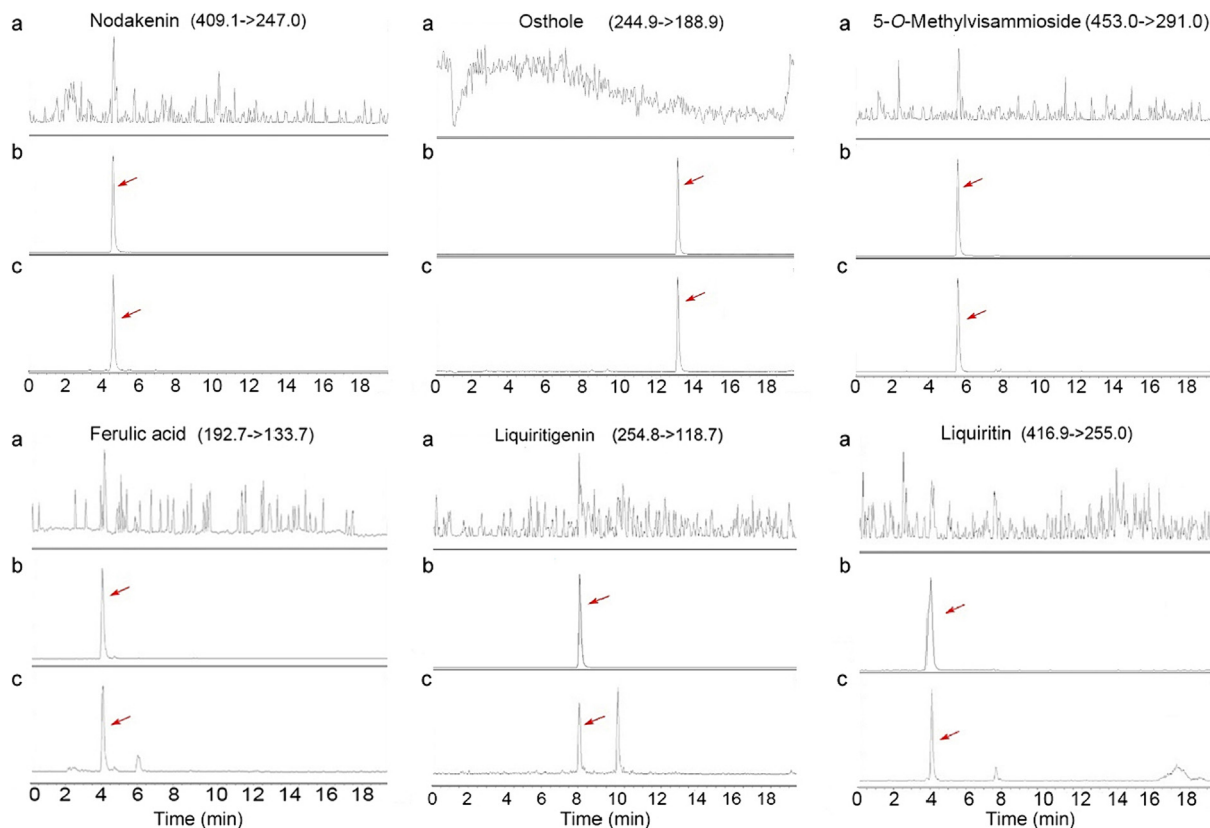
Fig. 1. Typical chromatogram of plasma samples for six components. (a) Blank plasma; (b) Blank plasma with mixed reference solution; (c) Plasma collected after oral administration 1 h.

Table 2
Linear regression data of six components.

Components	Regression equation	r	Linear range (ng/mL)	LLOQ (ng/mL)
Nodakenin	$y = 0.103\ 1x - 0.002\ 911$	0.999 5	1.050–1 075.2	1.050
Osthole	$y = 0.474\ 1x - 0.025\ 50$	0.996 0	1.281–1 312.0	1.281
5-O-Methylvisammioside	$y = 0.128\ 2x - 0.001\ 725$	0.999 8	0.556–569.6	0.556
Ferulic acid	$y = 0.001\ 787x + 1.232 \times 10^{-4}$	0.999 7	1.175–1 203.0	1.175
Liquiritigenin	$y = 0.024\ 25x + 4.273 \times 10^{-5}$	0.999 7	0.630–648.0	0.630
Liquiritin	$y = 0.022\ 97x - 2.269 \times 10^{-4}$	0.999 9	0.840–1 082.0	0.840

Table 3
Precision and accuracy results of six components in intra-day and inter-day.

Components	Concentrations (ng/mL)	Intra-day ($n = 6$)		Inter-day ($n = 3$)	
		RSD (%)	RE (%)	RSD (%)	RE (%)
Nodakenin	2.100	2.31	1.09	2.94	4.19
	537.6	1.78	−1.52	1.91	−7.26
	806.4	1.22	−0.99	1.71	−3.27
Osthole	2.562	1.59	−0.36	2.77	1.56
	656.0	2.65	−2.55	1.34	−6.94
	984.0	3.63	0.69	2.80	−6.27
5-O-Methylvisammioside	1.112	3.09	0.97	3.45	2.17
	284.8	3.67	−4.62	2.70	−3.29
	427.2	4.55	−2.55	3.75	−2.85
Ferulic acid	2.350	1.59	−0.46	2.89	−7.09
	601.6	5.85	−2.06	2.02	−6.01
	902.4	2.26	−3.58	1.23	−5.21
Liquiritigenin	1.260	3.54	1.45	4.40	2.57
	324.0	4.96	−1.12	1.79	−3.96
	486.0	2.82	−4.04	2.32	−4.72
Liquiritin	1.680	2.32	8.33	1.72	14.08
	541.0	4.55	−0.38	2.00	−2.16
	811.5	5.81	−4.29	2.83	−4.16

Table 4
Results of extraction recovery and matrix effect for six components (n = 6).

Components	Concentrations (ng/mL)	Matrix effect		Extraction recovery	
		Mean (%)	RSD (%)	Mean (%)	RSD (%)
Nodakenin	2.100	93.56	5.51	95.72	2.85
	537.6	95.95	3.07	93.20	5.80
	806.4	95.67	3.71	99.06	6.62
Osthole	2.562	71.48	2.07	107.01	3.68
	656.0	70.89	5.78	95.65	6.43
	984.0	72.81	5.70	90.64	4.68
5-O-Methylvisammioside	1.112	113.58	4.35	91.82	3.21
	284.8	109.28	4.65	89.19	3.50
	427.2	110.88	3.49	91.92	2.98
Ferulic acid	2.350	108.58	2.70	104.24	2.06
	601.6	99.85	1.68	91.54	1.55
	902.4	95.09	2.53	93.85	6.90
Liquiritigenin	1.260	95.91	4.21	99.30	4.09
	324.0	95.52	2.34	91.52	2.47
	486.0	95.74	0.91	92.19	4.75
Liquiritin	1.680	92.76	3.35	98.25	3.15
	541.0	95.73	5.22	92.34	4.73
	811.5	101.57	2.68	89.22	3.25

Table 5
Stability results of six components under different storage conditions (n = 6).

Components	Concentrations (ng/mL)	RE (%)		
		4 °C for 24 h	−80 °C for 5 d	Three-freeze–thaw cycles
Nodakenin	2.100	−4.74	−6.72	−5.56
	537.6	−9.40	−7.53	−4.04
	806.4	−6.52	6.84	−4.56
Osthole	2.562	2.33	12.26	7.23
	656.0	−3.73	4.02	2.14
	984.0	−5.16	−0.47	0.13
5-O-Methylvisammioside	1.112	−1.14	−3.87	−2.74
	284.8	−4.40	−6.12	−1.88
	427.2	−6.10	−5.65	−8.54
Ferulic acid	2.350	12.16	8.98	9.09
	601.6	−2.84	−2.23	−2.08
	902.4	−6.47	−5.63	−5.84
Liquiritigenin	1.260	0.57	9.00	8.20
	324.0	−12.01	1.97	5.41
	486.0	−7.02	0.22	2.47
Liquiritin	1.680	−0.69	2.44	4.35
	541.0	−5.67	−5.38	−2.67
	811.5	−4.78	−1.80	−6.84

used the LC-MS/MS method to quantitatively analyze the main constituents in QSD granules.

3.2. Pharmacokinetics study

Using the established LC-MS/MS method, the concentrations of nodakenin, osthole, 5-O-methylvisammioside, ferulic acid, liquiritigenin and liquiritin in plasma were determined in normal and RA rats after intragastric administration of QSD granules. The difference of the pharmacokinetics between normal and RA rats was discovered. The results of pharmacokinetic parameters were presented in Table 6, and the drug-time curves were illustrated in Fig. 2.

In comparison with the normal rats, the value of t_{max} and $AUC_{0-\infty}$ for nodakenin was significantly increased (P < 0.05) in the RA rats, which indicated that its absorption rate was significantly decreased, the absorptive amount *in vivo* was remarkably improved in the pathological state. Compared to the normal rats, the C_{max} of nodakenin was higher, the $t_{1/2}$ and the $MRT_{0-\infty}$ were decreased in the RA rats, indicating that the exposure concentration for nodakenin was greater, the elimination velocity was raised, the action time *in vivo* was reduced under the pathological state.

Nodakenin, in normal and RA rats, had the highest absorptive amount and the exposure concentration among the six compounds and it was related to its high content in the granules, and the results were consistent with a previous research (Hwang, Cho, Jang, Ha, & Ma, 2014). In contrast with the normal rats, for osthole, the t_{max} was later, the C_{max} was lower, the $AUC_{0-\infty}$ was increased, the $t_{1/2}$ became longer, and the $MRT_{0-\infty}$ was increased in the RA rats, indicating a lower absorption rate, a lower exposure concentration, a higher absorptive amount, a lower elimination velocity, and a longer retention time in the pathological state. Compared to the normal rats, the t_{max} of 5-O-methylvisammioside was later, the C_{max} was lower, the $AUC_{0-\infty}$ was increased, the $t_{1/2}$ became longer, and the $MRT_{0-\infty}$ was increased in the RA rats, which indicated that the absorption rate of 5-O-methylvisammioside was lower, the exposure concentration was lower, the absorptive amount was higher, the elimination velocity was decreased, and the retention time was raised in the body of RA rats. In addition, the t_{max} of ferulic acid was consistent in both groups and it showed that its absorption rate remained constant in two groups. Compared with the normal rats, the C_{max} of ferulic acid was lower, the $AUC_{0-\infty}$ and the $MRT_{0-\infty}$ were decreased, and the $t_{1/2}$ became longer in the RA rats, which implied that the exposure concentra-

Table 6
Pharmacokinetic parameters of six components in normal and RA groups after oral administration (mean ± SD, n = 6).

| Components	Groups	$t_{1/2}$ (h)	t_{max} (h)	C_{max} (ng/mL)	$AUC_{0-\infty}$ (h·ng/mL)	$MRT_{0-\infty}$ (h)
Nodakenin	Normal	8.26 ± 3.72	0.22 ± 0.15	684.77 ± 305.11	2 967.31 ± 617.45	9.82 ± 1.23
	RA	6.57 ± 0.92	0.79 ± 0.29*	747.72 ± 348.57	3 971.61 ± 643.91*	8.58 ± 1.68
Osthole	Normal	23.95 ± 10.06	0.08 ± 0.00	84.56 ± 51.09	187.34 ± 27.04	34.17 ± 13.48
	RA	52.89 ± 39.72	0.24 ± 0.37	39.75 ± 47.08	218.00 ± 84.60	70.02 ± 47.03
5-O-Methylvisammioside	Normal	16.00 ± 4.94	0.17 ± 0.05	32.40 ± 15.28	84.84 ± 12.44	22.28 ± 6.40
	RA	18.58 ± 6.00	0.22 ± 0.16	24.61 ± 18.08	94.48 ± 23.72	22.58 ± 3.33
Ferulic acid	Normal	3.57 ± 2.20	0.08 ± 0.00	480.45 ± 323.39	518.33 ± 181.72	6.39 ± 2.70
	RA	4.28 ± 1.07	0.08 ± 0.00	236.48 ± 232.97	362.80 ± 118.03	5.45 ± 1.56
Liquiritigenin	Normal	10.33 ± 1.79	2.07 ± 4.87	33.99 ± 18.30	144.73 ± 66.67	15.71 ± 1.81
	RA	10.60 ± 2.99	3.87 ± 5.04	18.27 ± 16.48	112.16 ± 34.95	16.37 ± 4.06
Liquiritin	Normal	11.18 ± 1.68	0.17 ± 0.05	63.13 ± 26.58	214.46 ± 38.77	18.14 ± 6.23
	RA	15.56 ± 6.81	0.25 ± 0.14	57.18 ± 35.47	225.74 ± 30.27	16.89 ± 2.58

Note: * denotes $P < 0.05$ *vs* normal group.
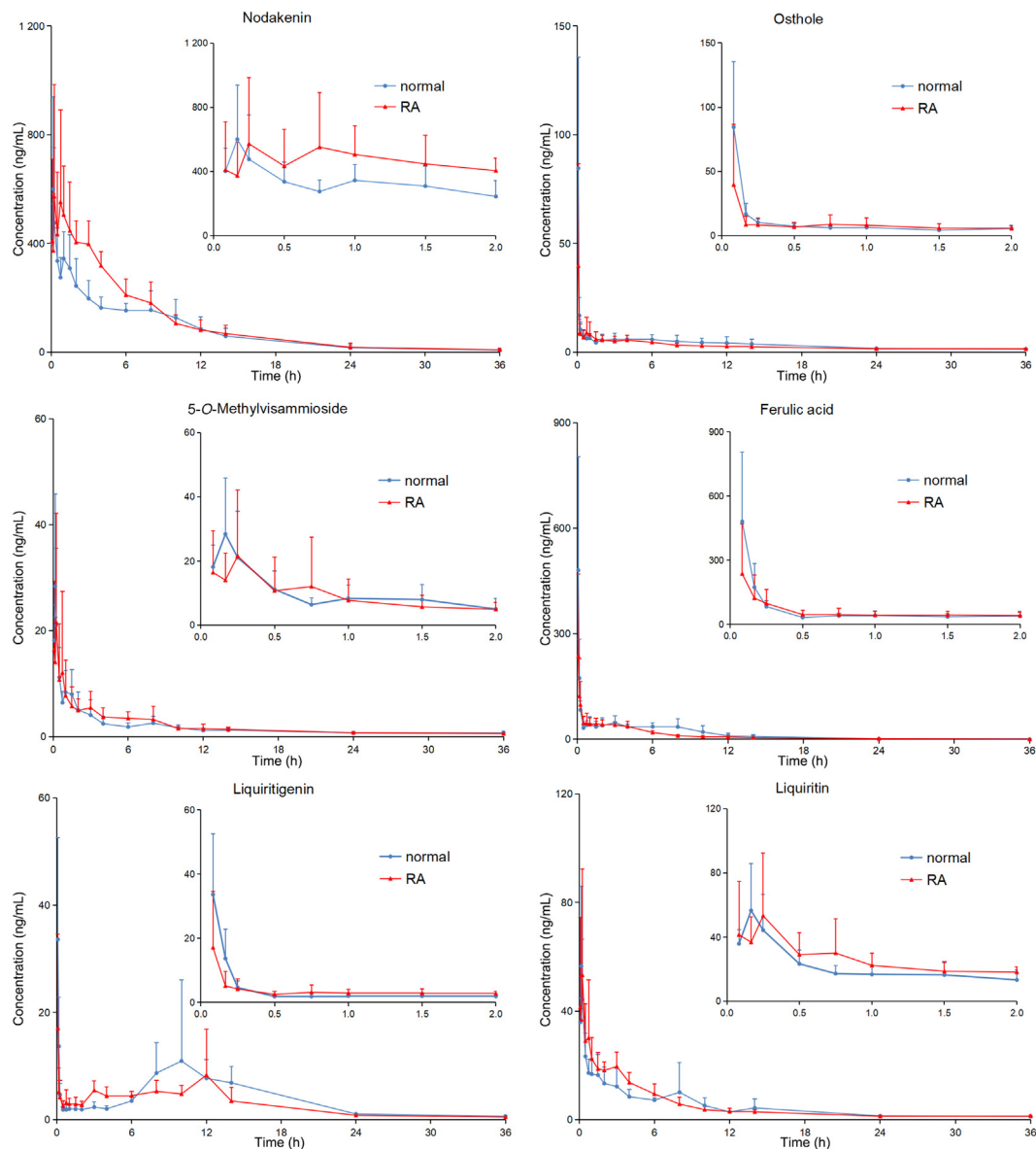
Fig. 2. Concentration-time curves of six components in normal and RA groups (mean ± SD, n = 6).

tion of ferulic acid was lower, the absorption value and the retention time were reduced *in vivo* under pathological conditions. In comparison with the normal rats, for liquiritigenin, the t_{max} was later, the C_{max} and the $AUC_{0-\infty}$ were lower, the $MRT_{0-\infty}$ was

increased, and the $t_{1/2}$ became longer in the RA rats, indicating a lower absorption rate, a lower exposure concentration, a lower absorption value, a higher retention time, and a lower elimination velocity *in vivo* in the RA rats. Notably, the bimodal phenomenon of

liquiritigenin was exhibited from the drug-time curve in normal and RA groups, which indicated that its metabolism *in vivo* might exist in enterohepatic circulation or reabsorption (Roberts, Magnusson, Burczynski, & Weiss, 2002). Moreover, Han et al. found that a portion of liquiritigenin was converted from liquiritin (Han, Kang, Yang, Choi, & Song, 2019), resulting in a raised concentration of liquiritigenin at 10–12 h. Compared to the normal rats, the t_{max} of liquiritin for RA rats was later, the C_{max} was lower, the $AUC_{0-\infty}$ was increased, the $t_{1/2}$ became longer, and the $MRT_{0-\infty}$ was increased, and the date demonstrated that the absorption rate of liquiritin was lower, the exposure concentration was lower, the absorptive amount of liquiritin was higher, the elimination velocity was decreased, and the retention time was raised in the RA rats.

4. Discussion

According to the above results, there were differences in the pharmacokinetic behavior of QSD granules in healthy and pathological states. The reasons for these differences require further research. Zhang et al. found that nodakenin exerts anti-inflammatory activity due to its excellent affinity with the protein core target "prostaglandin-endoperoxide synthase 2 (PTGS2)" through the network pharmacological technique (Zhang et al., 2023). In addition, nodakenin can inhibit the phosphorylation of transforming growth factor β (TGF-β)-activated kinase (TAK)-1, and inhibit the transcription of nuclear factor-κB (NF-κB) and the production of pro-inflammatory mediators in the inflammatory liver injury model (Lim, Lee, Yun, Lee, & Kim, 2021). Based on research of Bao et al, osthole can inhibit the production of the inflammatory cytokines tumor necrosis factor (TNF)–α, interleukin (IL)–6 and IL–1β, and play a part in anti–inflammatory effects via the NF-κB and nuclear factor erythroid 2–related factor 2 (Nrf2) pathways (Bao et al., 2018). Meng et al. found that 5-*O*-methylvisammioside can be anti-inflammatory by reducing the amount of IL–1β, IL–6 and toll like receptor 4 (TLR4) in inflammatory RAW264.7 cells (Meng, Gao, Liu, Zheng, & Jia, 2023). Moreover, 5-*O*-methylvisammioside can reduce the amount of malondialdehyde (MDA), increase superoxide dismutase (SOD) activity, down-regulate expression levels of TNF–α and IL–1β protein in inflammatory colon cells, and then improve the inflammation (Meng, Gao, Liu, Zheng, & Jia, 2023). Ferulic acid can have an anti-inflammatory effect by regulating NF-κB's activity, P38 MAPK pathway, and the levels of peroxisome proliferator activated receptors (PPAR γ) agonist and cell adhesion molecules (CAM) (Li et al., 2021). Jiang et al. discovered that inducible nitric oxide synthase (iNOS) target protein may be the key to exerting anti-inflammatory function for Gancao, and two components, liquiritigenin and liquiritin, show remarkable inhibitory effects on the expression of iNOS protein (Jiang et al., 2022). Moreover, it was found that QSD may exert anti-inflammatory effect via MAPKs/CREB signaling pathway (Hu et al., 2022).

RA is a chronic, extremely complex inflammatory disease, and the protein kinases are the key to achieve signal transduction in inflammatory pathways (Jiang et al., 2022; Gaestel, Kotlyarov, & Kracht, 2009). The pharmacokinetic behavior of drug is particularly affected by the proteins in the ATP-binding cassette (ABC) and solute carrier (SLC) superfamilies (Cressman, Petrovic, & Piquette-Miller, 2012). In addition, inflammation could regulate the expression of related protein transporters on the cell membrane, change the permeability of the cell membrane, and these made the difference in the absorption, distribution, metabolism and elimination of drugs (Cressman et al., 2012). Some studies had shown that the pathological state would affect the expression of metabolic enzymes, and thus the pharmacokinetics behavior of drugs was changed *in vivo* (Nakai et al., 2008; Zgheib, & Branch, 2017; Zanger, Klein, Richter, Toscano, & Zukunft, 2005). Although the pharmacokinetics of QSD granules in normal rats and RA rats has been studied and analyzed in this research, it was a single dose, and the pharmacokinetics in rats given multiple dosing has not been explored. The pharmacodynamic study is an indispensable part of the study on the mechanism of drug action and clinical efficacy. Therefore, QSD granules can be further explore by studying the pharmacokinetics and pharmacodynamics of multiple administration.

5. Conclusion

In this study, a bioanalytical method, based on LC-MS/MS analysis, was developed and fully validated to quantify six components of QSD granules in rats' plasma. The method was further applied to analyze the plasma samples of rats treated with QSD granules. Furthermore, the study was conducted to compare the pharmacokinetic differences of QSD granules in normal and RA rats, which could demonstrate the pharmacokinetic characteristics of multiple components and reflect the possible interactions among the components in QSD. This study provided scientific and valuable data for the mechanism study and clinical application of QSD granules.

CRediT authorship contribution statement

Xin Li: Data curation, Formal analysis, Visualization, Writing – original draft. **Min Wang:** Data curation, Formal analysis, Visualization, Writing – original draft. **Yuhong Zhong:** Writing – review & editing. **Qianqian Yin:** Writing – review & editing. **Zheming Hu:** Writing – review & editing. **Wenli Tian:** Writing – review & editing. **Zhongyan Liu:** Conceptualization. **Zhidong Liu:** Project administration, Supervision, Writing – review & editing.

Declaration of Competing Interest

The authors declare that they have no known competing financial interests or personal relationships that could have appeared to influence the work reported in this paper.

Acknowledgments

References

Bao, Y. X., Meng, X. L., Liu, F. N., Wang, F., Yang, J. H., Wang, H. Y., & Xie, G. H. (2018). Protective effects of osthole against inflammation induced by lipopolysaccharide in BV2 cells. *Molecular Medicine Reports, 17*(3), 4561–4566.

Chen, M. W., Zhang, C. C., Zhang, J. N., Kai, G. Y., Lu, B., Huang, Z. L., & Ji, L. L. (2019). The involvement of DAMPs-mediated inflammation in cyclophosphamide-induced liver injury and the protection of liquiritigenin and liquiritin. *European Journal of Pharmacology, 856*, 172421.

Cui, T. C., Hou, Y. Z., Feng, H. M., Wu, S. J., Li, W. L., & Li, Z. (2022). Granulation process analysis technologies and potential applications in traditional Chinese medicine. *Acupuncture and Herbal Medicine, 2*(1), 9–24.

Cressman, A. M., Petrovic, V., & Piquette-Miller, M. (2012). Inflammation-mediated changes in drug transporter expression/activity: Implications for therapeutic drug response. *Expert Review of Clinical Pharmacology, 5*(1), 69–89.

Dong, Y., Hou, Y. J., Li, S. S., Liu, S. H., Li, B., Li, B., Gao, J., & Shang, Q. (2018). Analysis of Qianghuo Shengshitang based on ancient literatures. *Chinese Journal of Experimental Traditional Medical Formulae, 24*(17), 1–5.

Gao, Q. T., Jeon, S. J., Jung, H. A., Lee, H. E., Park, S. J., Lee, Y., Lee, Y., Ko, S. Y., Kim, B., Choi, J. S., & Ryu, J. H. (2015). Nodakenin enhances cognitive function and adult hippocampal neurogenesis in mice. *Neurochemical Research, 40*(7), 1438–1447.

Gaestel, M., Kotlyarov, A., & Kracht, M. (2009). Targeting innate immunity protein kinase signalling in inflammation. *Nature Reviews Drug Discovery, 8*(6), 6.

He, Y. F., Mai, C. T., Pan, H. D., Liu, L., Zhou, H., & Xie, Y. (2021). Targeting immunometabolism by active ingredients derived from traditional Chinese medicines for treatment of rheumatoid arthritis. *Chinese Herbal Medicines, 13*(4), 451–460.

Hu, N., Wang, C. H., Wang, B. H., Wang, L. B., Huang, J., Wang, J. H., & Li, C. L. (2022). Qianghuo Shengshi decoction exerts anti-inflammatory and analgesic via MAPKs/CREB signaling pathway. *Journal of Ethnopharmacology, 284*, 114776.

Hwang, Y. H., Cho, W. K., Jang, D., Ha, J. H., & Ma, J. Y. (2014). High-performance liquid chromatography determination and pharmacokinetics of coumarin compounds after oral administration of Samul-Tang to rat. *Pharmacognosy Magazine, 10*(37), 34–39.

Han, Y. J., Kang, B., Yang, E. J., Choi, M. K., & Song, I. S. (2019). Simultaneous determination and pharmacokinetic characterization of glycyrrhizin, isoliquiritigenin, liquiritigenin, and liquiritin in rat plasma following oral administration of *Glycyrrhizae Radix* extract. *Molecules, 24*(9), 1816.

Jiang, X. J., Lin, Y. H., Wu, Y. L., Yuan, C. X., Lang, X. L., Chen, J. Y., Zhu, C. Y., Yang, X. Y., Huang, Y., Wang, H., & Wu, C. S. (2022). Identification of potential anti-pneumonia pharmacological components of *Glycyrrhizae Radix* et *Rhizoma* after the treatment with Gan An He Ji oral liquid. *Journal of Pharmaceutical Analysis, 12*(6), 839–851.

Kim, T. W. (2023). Nodakenin induces ROS-dependent apoptotic cell death and ER stress in radioresistant breast cancer. *Antioxidants, 12*(2), 492.

Lim, J. Y., Lee, J. H., Yun, D. H., Lee, Y. M., & Kim, D. K. (2021). Inhibitory effects of nodakenin on inflammation and cell death in lipopolysaccharide-induced liver injury mice. *Phytomedicine, 81*, 153411.

Liao, Y., Xiao, L., Li, J. C., Tan, R. Z., Xia, Z., & Wang, L. (2020). Nodakenin alleviates renal ischaemia-reperfusion injury via inhibiting reactive oxygen species-induced NLRP3 inflammasome activation. *Nephrology, 26*(1), 78–87.

Liu, Y. W., Chiu, Y. T., Fu, S. L., & Huang, Y. T. (2015). Osthole ameliorates hepatic fibrosis and inhibits hepatic stellate cell activation. *Journal of Biomedical Science, 22*(1), 63.

Li, D., Rui, Y. X., Guo, S. D., Luan, F., Liu, R., & Zeng, N. (2021). Ferulic acid: A review of its pharmacology, pharmacokinetics and dervatives. *Life Science, 284*, 119921.

Lee, K. K., Omiya, Y., Yuzurihara, M., Kase, Y., & Kobayashi, H. (2013). Antispasmodic effect of shakuyakukanzoto extract on experimental muscle cramps *in vivo*: Role of the active constituents of *Glycyrrhizae Radix. Journal of Ethnopharmacology, 145*(1), 286–293.

Lin, M. N. (2019). Comparative study on modern application of traditional Chinese medicine decotion and traditional Chinese medicine granule. *Chinese Community Doctors, 35*(34), 100–101.

Li, Y. Z., Wang, Y. L., Tai, W., Yang, L., Chen, Y., Chen, C. Q., & Liu, C. X. (2015). Challenges and solutions of pharmacokinetics for efficacy and safety of traditional Chinese medicine. *Current Drug Metabolism, 16*(9), 756–776.

Liu, W. Y., Zeng, K. Q., Zhou, X., Zhang, Y. F., & Nie, C. (2022). Comparative study on brain pharmacokinetics of Buyang Huanwu decoction in normal and cerebral ischemia rats using brain microdialysis combined with LC-MS/MS. *Chinese Herbal Medicines, 14*(4), 630–637.

Ma, R. J., Maharajan, K. N., Zhuang, K. Y., Xia, Q., Sun, D., Tu, P. F., Fan, T. P., Liu, K. C., & Zhang, Y. (2023). Pharmacological importance of Kunxian capsule in clinical applications and its adverse effects: A review. *Chinese Herbal Medicines, 15*(2), 222–230.

Meng, N., Lyu, Y., Zhang, X. Y., Chai, X., Li, K. F., & Wang, Y. F. (2022). The exciting and magical journey of components from compound formulae to where they fight. *Acupuncture and Herbal Medicine, 2*(4), 240–252.

Meng, L., Gao, L. M., Liu, X. H., Zheng, W., & Jia, T. Z. (2023). Study on anti-inflammatory effect and mechanism of 4′-O-β-D-glucosyl-5-O-methylvisamminol in *Radix Saposhnikoviae. Chinese Archives of Traditional Chinese Medicine, 41*(4).

Meng, F. C., & Lin, J. K. (2019). Liquiritigenin inhibits colorectal cancer proliferation, invasion, and epithelial-to-mesenchymal transition by decreasing expression of runt-related transcription factor 2. *Oncology Research Featuring Preclinical and Clinical Cancer Therapeutics, 27*(2), 139–146.

Nakai, K., Tanaka, H., Hanada, K., Ogata, H., Suzuki, F., Kumada, H., Miyajima, A., Ishida, S., Sunouchi, M., Habano, W., Kamikawa, Y., Kubota, K., Kita, J., Ozawa, S., & Ohno, Y. (2008). Decreased expression of cytochromes P450 1A2, 2E1, and 3A4 and drug transporters Na⁺-taurocholate-cotransporting polypeptide, organic cation transporter 1, and organic anion-transporting peptide-C correlates with the progression of liver fibrosis in chronic hepatitis C patients. *Drug Metabolism and Disposition, 36*(9), 1786–1793.

Ren, Z. L., Lv, M., & Xu, H. (2022). Osthole: Synthesis, structural modifications, and biological properties. *Mini-reviews in Medicinal Chemistry, 22*(16), 2124–2137.

Roberts, M. S., Magnusson, B. M., Burczynski, F. J., & Weiss, M. (2002). Enterohepatic Circulation: Physiological, pharmacokinetic and clinical implications. *Clinical Pharmacokinetics, 41*(10), 751–790.

Smolen, J. S., Aletaha, D., & McInnes, I. B. (2016). Rheumatoid arthritis. *The Lancet, 388*(10055), 2023–2038.

Sun, X. L., Zhang, T. W., Zhao, Y., Cai, E. B., Zhu, H. Y., & Liu, S. L. (2020). The protective effect of 5-O-methylvisammioside on LPS-induced depression in mice by inhibiting the over activation of BV-2 microglia through Nf-κB/IκB-α pathway. *Phytomedicine, 79*, 153348.

Wang, L., Liang, R. X., Cao, Y., & Ye, J. X. (2008). Effect of prim-O-glucosylcimifugin and 4′-O-β-D-glucosyl-5-O-methylvisa-mminol con on proliferation of smooth muscle cell stimulated by TNF-α. *China Journal of Chinese Materia Medica, 2008* (17), 2157–2160.

Wei, F., Jiang, X., Gao, H. Y., & Gao, S. H. (2017). Liquiritin induces apoptosis and autophagy in cisplatin (DDP)-resistant gastric cancer cells *in vitro* and xenograft nude mice *in vivo. International Journal of Oncology, 51*(5), 1383–1394.

Xie, Y., Mai, C. T., Zheng, D. C., He, Y. F., Feng, S. L., Li, Y. Z., Liu, C. X., Zhou, H., & Liu, L. (2021). Wutou decoction ameliorates experimental rheumatoid arthritis via regulating NF-KB and Nrf 2: Integrating efficacy-oriented compatibility of traditional Chinese medicine. *Phytomedicine, 85*, 153522.

Xu, Z. R., Jiang, C. H., Fan, S. Y., Yan, R. J., Xie, N., & Wu, C. Z. (2019). Comparative pharmacokinetics of naringin and neohesperidin after oral administration of flavonoid glycosides from *Aurantii Fructus Immaturus* in normal and gastroontestinal motility disorders mice. *Chinese Herbal Medicines, 11*(3), 314–320.

Yi, N., Mi, Y. L., Xu, X. T., Li, N. P., Chen, B. Y., Yan, K., Tan, K. Y., Zhang, B., Wang, L. H., Kuang, G. Y., & Lu, M. (2022). Nodakenin attenuates cartilage degradation and inflammatory responses in a mice model of knee osteoarthritis by regulating mitochondrial Drp1/ROS/NLRP3 axis. *International Immunopharmacology, 113*, 109349.

Yang, Y. Q., Zhu, R. C., Li, J., Yang, X. J., He, J., Wang, H., & Chang, Y. X. (2019). Separation and enrichment of three coumarins from *Angelicae Pubescentis Radix* by macroporous resin with preparative HPLC and evaluation of their anti-inflammatory activity. *Molecules, 24*(14), 2664.

Zhang, W., Sun, Y. F., Jin, C. S., Gao, B., Ren, C. J., & Zhao, H. S. (2022a). Research status and prospect of traditional Chinese medicine formula granules. *Chinese Traditional and Herbal Drugs, 53*(22), 7221–7233.

Zhang, X. P., Bai, L., Feng, S. F., & Miao, M. S. (2022b). Medication regularity of Chinese medicine in treatment of rheumatoid arthritis based on date mining. *Pharmacology and Clinics of Chinese Materia Medica*, 1–14.

Zhang, Y. X., Zhang, J. G., HAmamozhi, A., Li, L., Yang, Z. J., & Zhang, Z. F. (2023). Excavation and resource evaluation of anti-inflammatory quality markers of *Notopterygii Rhizoma* et *Radix. Chinese Traditional and Herbal Drugs, 54*(2), 652–662.

Zhang, X. J., Chen, J. H., Luo, L., He, W., Liu, G. H., Gong, J., Zeng, Y. F., Xie, Z. Y., & Liao, Q. F. (2018). Comparative brain pharmacokinetic study of Jiaotai pills in normal and insomnic rats using brain microdialysis combined with LC–MS/MS. *Chinese Herbal Medicines, 10*(2), 206–214.

Zgheib, N. K., & Branch, R. A. (2017). Drug metabolism and liver disease: A drug-gene-environment interaction. *Drug Metabolism Reviews, 49*(1), 35–55.

Zanger, U. M., Klein, K., Richter, T., Toscano, C., & Zukunft, J. (2005). Impact of genetic polymorphism in relation to other factors on expression and function of human drug-metabolizing P450. *Toxicology Mechanisms and Methods, 15*(2), 121–124.